Supplementary data

Revisiting the K-Mn-O System for Green Cathode Materials in Potassium ion Batteries: From K_2MnO_4 to K_3MnO_4

Armance Sagot,[a,c] Lorenzo Stievano,[b,c] Vadim M. Kovrugin,[a c] Tanguy Soudant,[a, c] and Valerie Pralong,[,a,c]*

[a] *Laboratoire de Cristallographie et Sciences des Matériaux CRISMAT, ENSICAEN, Université de Caen, CNRS, 6 Bd Maréchal Juin, F-14050 Caen, France.*

[b] *Institut Charles Gerhardt Montpellier, UMR 5253, CNRS, Université Montpellier, ENSCM, Montpellier 34095, France.*

[c] *Réseau sur le Stockage Electrochimique de l'Énergie (RS2E), FR CNRS 3459, 80039 Amiens, France.*

Abstract:

This study presents the synthesis, structural characterization, and electrochemical evaluation of α-K_3MnO_4 and K_2MnO_4 as potential cathode materials for potassium-ion batteries (KIBs). A new solid-state method was employed to prepare K_2MnO_4 from equimolar $KMnO_4$ and K_3MnO_4. Both phases contain isolated MnO_4 tetrahedra, but differ in potassium diffusion behaviour, as shown by bond valence energy landscape calculations. Electrochemical cycling demonstrates a reversible redox couple Mn^{6+}/Mn^{5+} at an average voltage of 2.4 V vs. K^+/K, delivering reversible capacities up to 110 mAh/g. *Operando* XRD and XAS confirm phase transitions and provide insights into structural and electronic evolution, including partial decomposition at high voltages. These findings demonstrate the potential of the K–Mn–O system for high-voltage, Mn-based KIB cathodes materials for KIBs.

Number of pages: 9
Number of figures: 7
Number of tables: 4

Table of contents

Crystallographic data
Rietveld refinements of the powder X-ray diffraction (PXRD) data for K_3MnO_4 and K_2MnO_4. S3
Crystallographic data for alpha-K_3MnO_4 and K_2MnO_4. S4
Fractional atomic coordinates and isotropic displacement parameters ($Å^2$) for alpha-K_3MnO_4. S4
Fractional atomic coordinates and isotropic displacement parameters ($Å^2$) for K_2MnO_4. S4

Characterizations
Magnetic susceptibility curves for K_3MnO_4 and K_2MnO_4. S5
Le Bail refinement of the post-mortem active material after 32 cycles at 3.2 V. S6

Electrochemical analysis
Discharge capacity of K_2MnO_4 as a function of cycle number. S6
Average charge and discharge potentials of K_2MnO_4 as a function of C-rate. S7

EXAFS analysis
Refined EXAFS parameters of each principal component related to the operando XAS dataset. S7
EXAFS fits of the pure components shown in real space. S8
EXAFS fits of the pure components dataset shown in the k space. S9

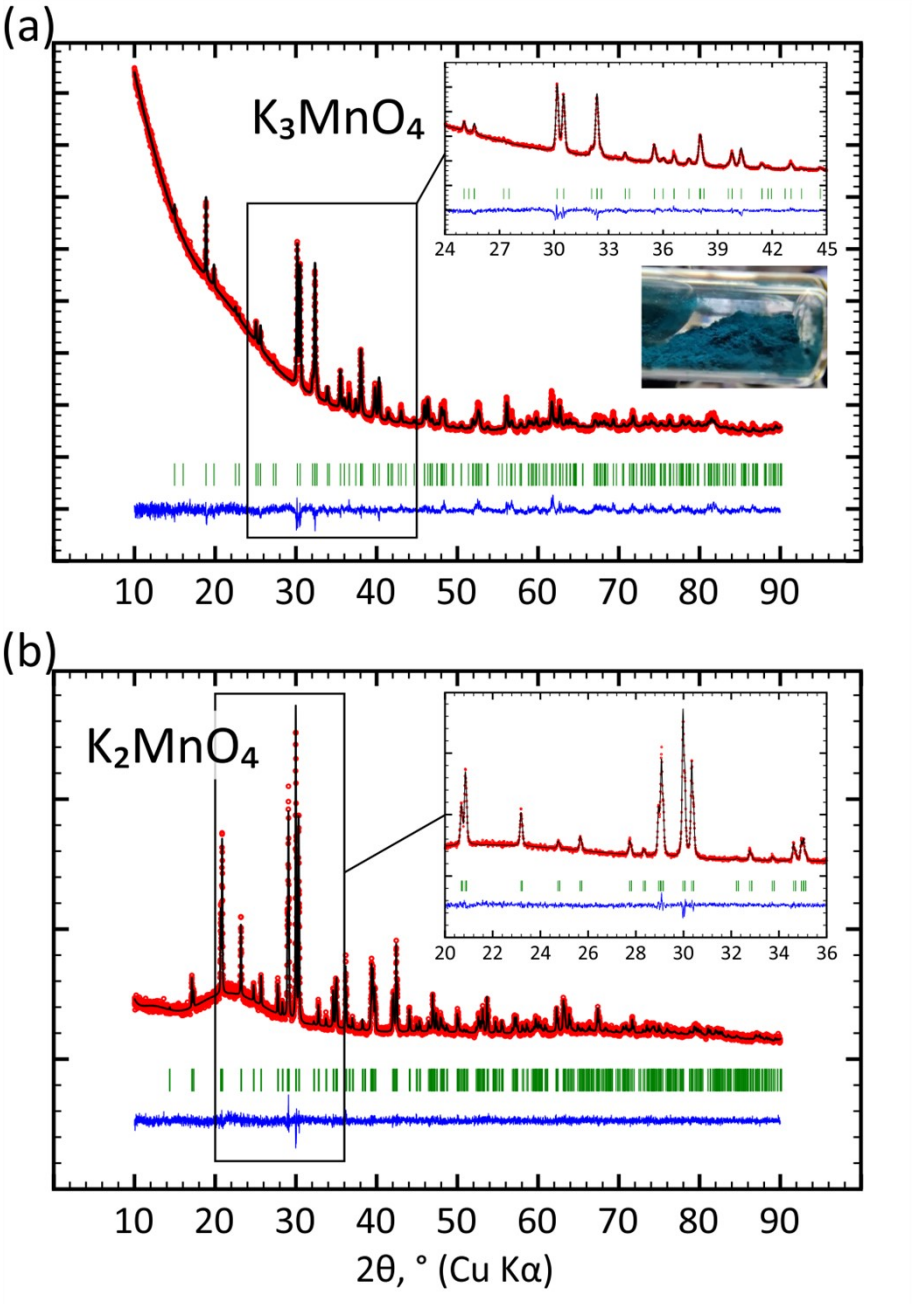

Figure S1: Rietveld refinements of the powder X-ray diffraction (PXRD) data for (a) K_3MnO_4 and (b) K_2MnO_4. The observed patterns are shown as red circles, the calculated profiles as black lines, and the difference curves as blue lines. Vertical green tick marks indicate the expected Bragg reflection positions. Panel (a) also includes a photograph of the synthesized duck-blue K_3MnO_4 powder. Refined unit cell parameters: (a) sp. gr. *Pnma*, *a* = 7.7492(6) Å, *b* = 8.9524(6) Å, *c* = 7.9053(5) Å, V = 548.42(7) Å^3; (b) sp. gr. *Pnma*, *a* = 7.6689(2) Å, *b* = 5.8872(1) Å, *c* = 10.3589(2) Å, and V = 467.68(2) Å^3.

Table S1: Crystallographic data for alpha-K_3MnO_4 and K_2MnO_4

	alpha-K_3MnO_4	K_2MnO_4
Space group	Orthorhombic, *Pnma*	Orthorhombic, *Pnma*
a, Å	7.7492(6)	7.66889(15)
b, Å	8.9524(6)	5.88719(11)
c, Å	7.9053(5)	10.3589(2)
Vol., Å^3	548.42(7)	467.68(2)
Z	2	4
D_x, g/cm^3	2.861	2.800
R_p, %	3.16	4.34
R_{wp}, %	5.09	5.49
GOF	1.95	0.95
χ^2	3.80	0.90

Table S2: Fractional atomic coordinates and isotropic displacement parameters (Å^2) for alpha-K_3MnO_4

Atom	*Wyck.*	*x*	*y*	*z*	U_{iso}
K1	4*c*	0.1681(12)	1/4	0.5537(11)	0.050(1)
K2	8*d*	0.4507(8)	0.0415(5)	0.2705(10)	0.0396(9)
Mn1	4*c*	0.2262(9)	1/4	0.0070(10)	0.0456(8)
O1	4*c*	0.202(3)	1/4	0.250(3)	0.0608(12)
O2	8*d*	0.160(2)	0.5627(18)	0.443(3)	0.0972(13)
O3	4*c*	−0.004(3)	1/4	0.897(3)	0.0448(9)

Table S3: Fractional atomic coordinates and isotropic displacement parameters (Å^2) for K_2MnO_4

Atom	*Wyck.*	*x*	*y*	*z*	U_{iso}
K1	4*c*	0.1641(3)	1/4	0.0871(3)	0.0111(14)
K2	4*c*	−0.0130(4)	1/4	0.6980(3)	0.0045(14)
Mn1	4*c*	0.2307(3)	1/4	0.4209(3)	0.0041(11)
O1	4*c*	0.0170(10)	1/4	0.4161(8)	0.022(3)
O2	4*c*	0.3045(11)	1/4	0.5719(9)	0.0029(12)
O3	8*d*	0.3052(8)	0.0162(11)	0.3468(5)	0.012(2)

Magnetic susceptibility

Magnetic susceptibility measurements performed with a magnetic field of 0.5 T between 5 and 400 K revealed a paramagnetic behaviour without long-range ordering in the whole temperature range for both compounds, α– and γ–K_3MnO_4. The interpolation of the experimental data using the Curie-Weiss law provides effective magnetic moments of $\mu_{eff}(\alpha)$=2.97 μ_B and $\mu_{eff}(\gamma)$=3.10 μ_B, slightly larger than the expected value μ_{eff} = 2.83 μB/Mn corresponding to the d^2 configuration of the Mn^{+V} oxidation state. This slight difference may be explained by possible experimental errors in weighing the sample or to the unlikely contamination during sample placement in the squid.

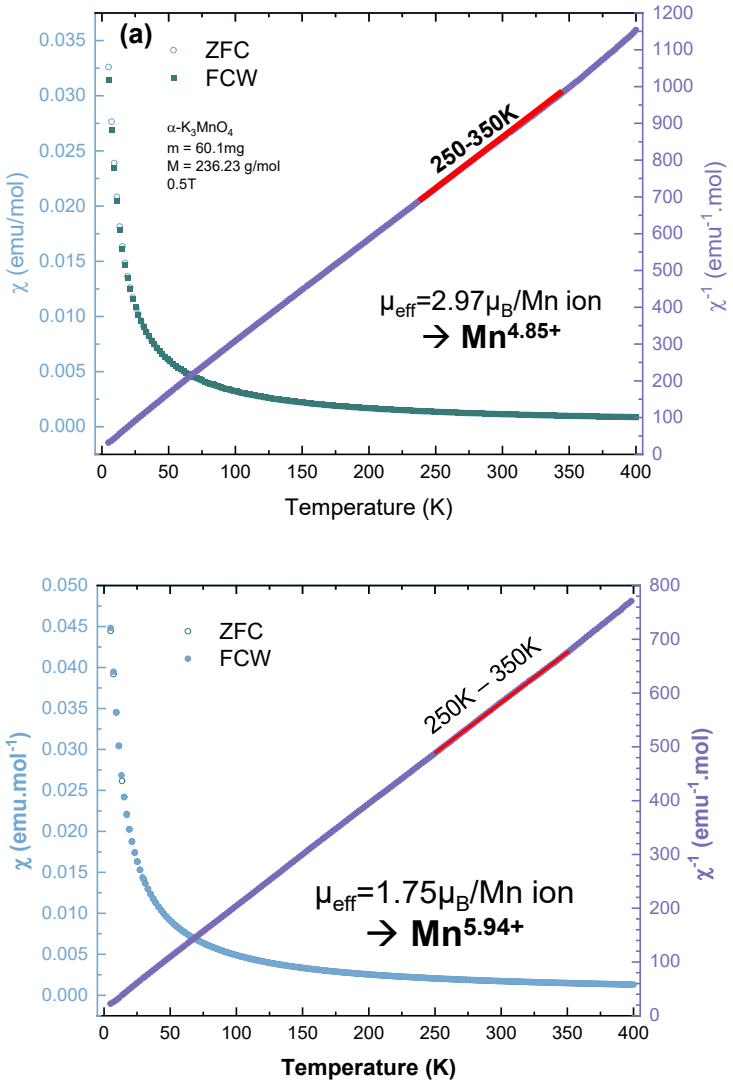

Figure S2: Magnetic susceptibility vs temperature under a 0.5T field between 5 and 400 K with inverse of the magnetic susceptibility of the FCW curve allowing linear regression in the paramagnetic range from 250 to 350K for (a) α – K_3MnO_4 and (b) K_2MnO_4.

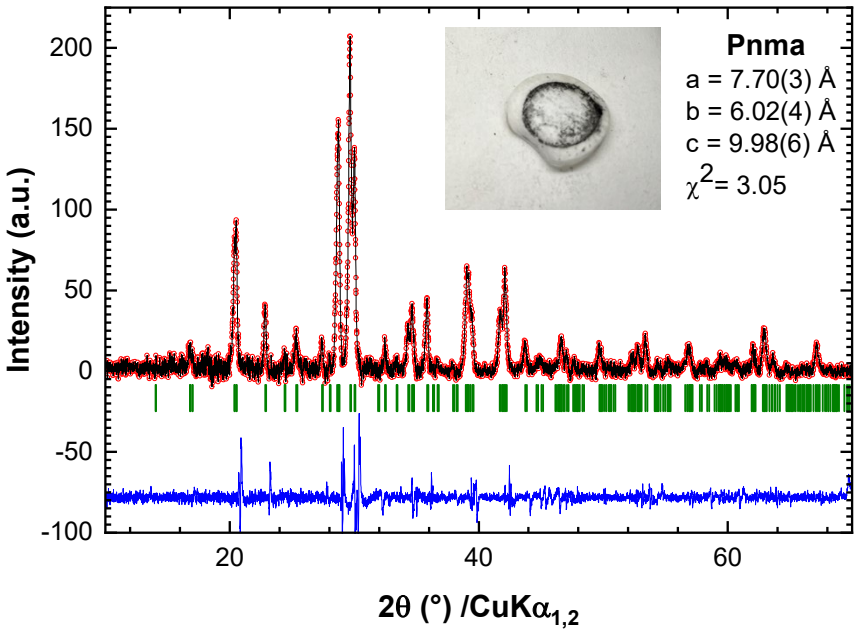

Figure S3: Le Bail refinement of the post-mortem active material after 32 cycles at 3.2 V. Inset: photograph of the cell separator.

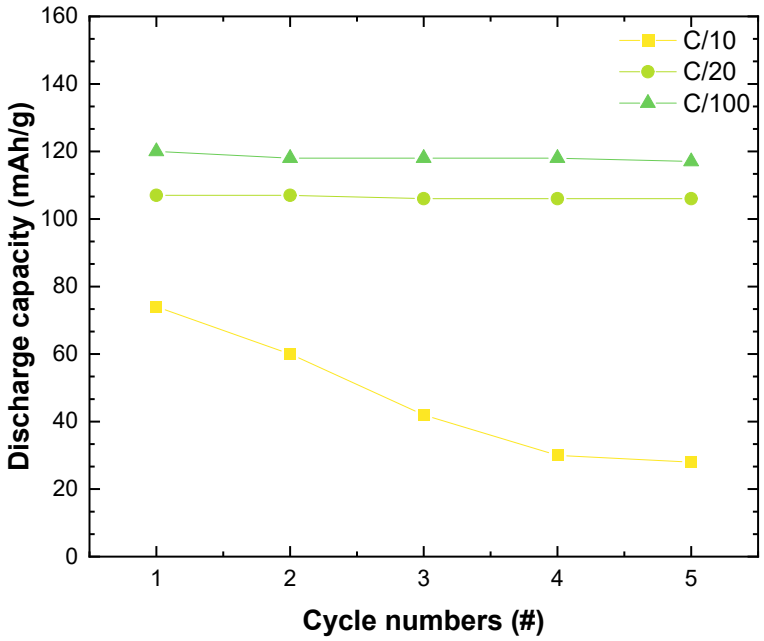

Figure S4: Discharge capacity of K_2MnO_4 as a function of cycle number at three different C-rates: C/10 (yellow), C/20 (light green), and C/100 (green), cycled vs. K in the 1.5–3.2 V window.

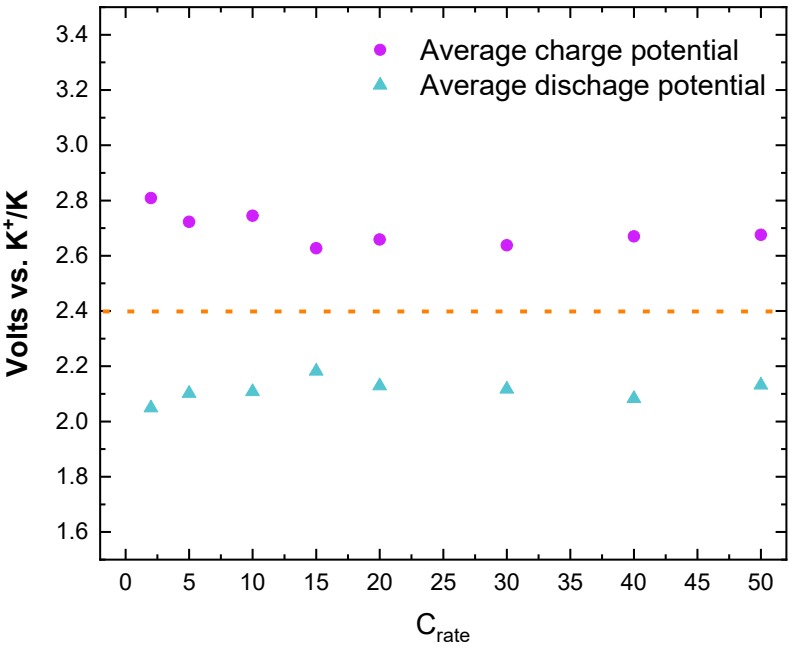

Figure S5: Average charge (magenta) and discharge (cyan) potentials of K_2MnO_4 as a function of C-rate.

Table S4: Refined EXAFS parameters of each principal component related to the operando XAS dataset for the discharge and charge of K II K_2MnO_4 electrochemical cell.

	Component		Bond	N	R (Å)	Debye-Waller Factor (10^{-3} Å^2)	Relative intensity
Discharge	Component 1	K_2MnO_4	Mn – O	4	1.62 (1)	2.6 (6)	
			Mn – K1	3	3.39 (9)	12.1 (6)	
			Mn – K2	2	3.61 (2)	15.3 (2)	
	Component 2	α - K_3MnO_4	Mn – O	4	1.65 (7)	1.3 (1)	
			Mn – K1	2	3.0 (3)	10.6 (4)	
			Mn – K3	6	3.41 (8)	10.6 (4)	
Charge	Component 1	α - K_3MnO_4	Mn – O	4	1.66 (6)	0.6 (1)	
			Mn – K1	2	2.98 (3)	11.9 (5)	
			Mn – K3	6	3.40 (8)	11.9 (5)	
	Component 2	K_2MnO_4	Mn – O	4	1.61 (1)	2.5 (8)	
			Mn – K1	3	3.36 (1)	11.4 (3)	
			Mn – K2	2	3.59 (6)	11.4 (3)	
	Component 3	MnO	Mn – O	6	2.25 (3)	2.6 (1)	0.68
			Mn – Mn	12	3.17 (3)	0.1 (2)	
		K_2MnO_4	Mn – O	4	1.58 (8)	2.6 (1)	0.32
	Component 4	MnO	Mn – O	6	2.32 (1)	0.3 (2)	0.51
			Mn – Mn	12	3.17 (0)	7.4 (2)	
		K_2MnO_4	Mn – O	4	1.65 (2)	0.3 (2)	0.49

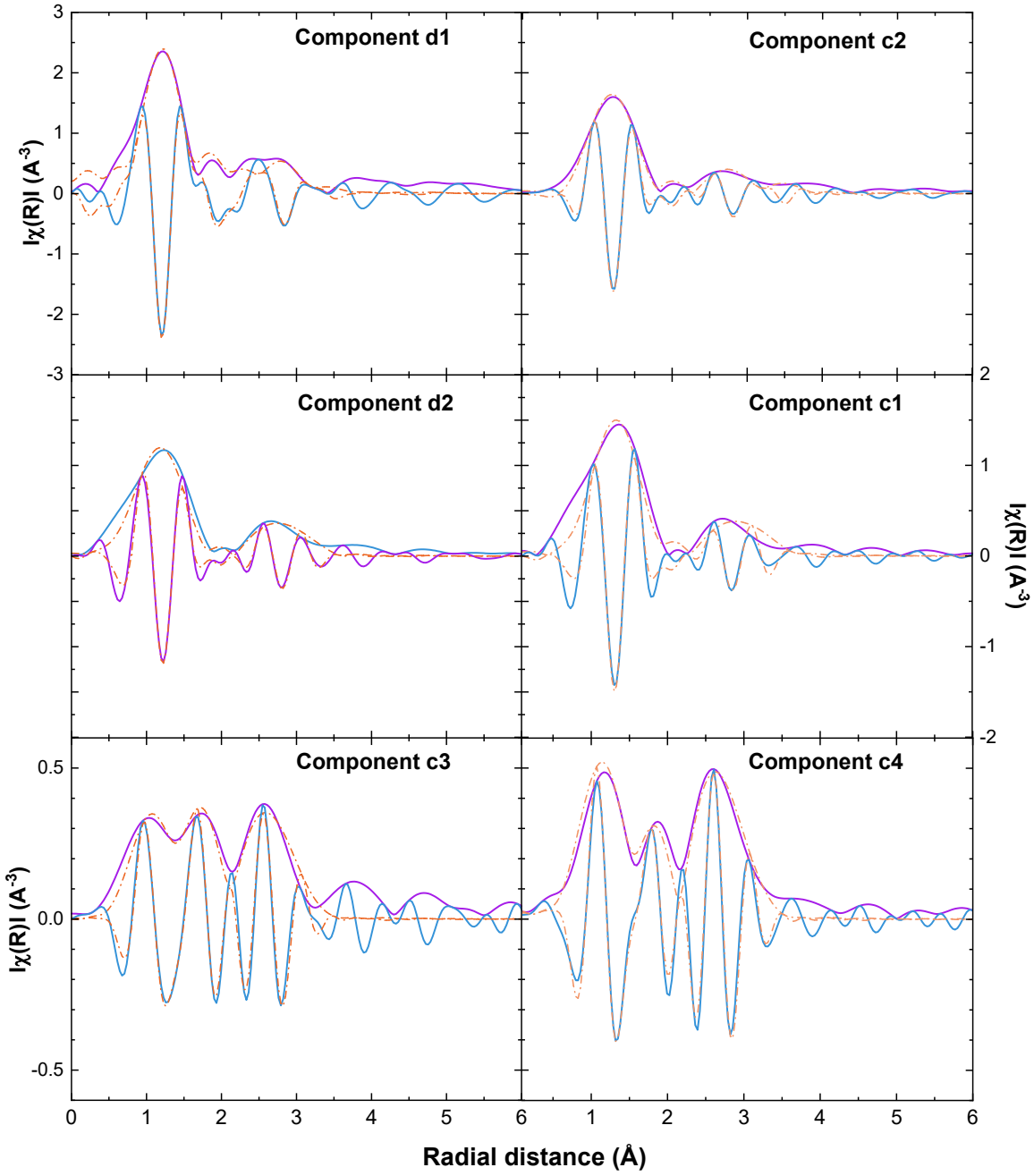

Figure S6: EXAFS fits of the pure components obtained from MCR-ALS analysis of the operando dataset shown in real space

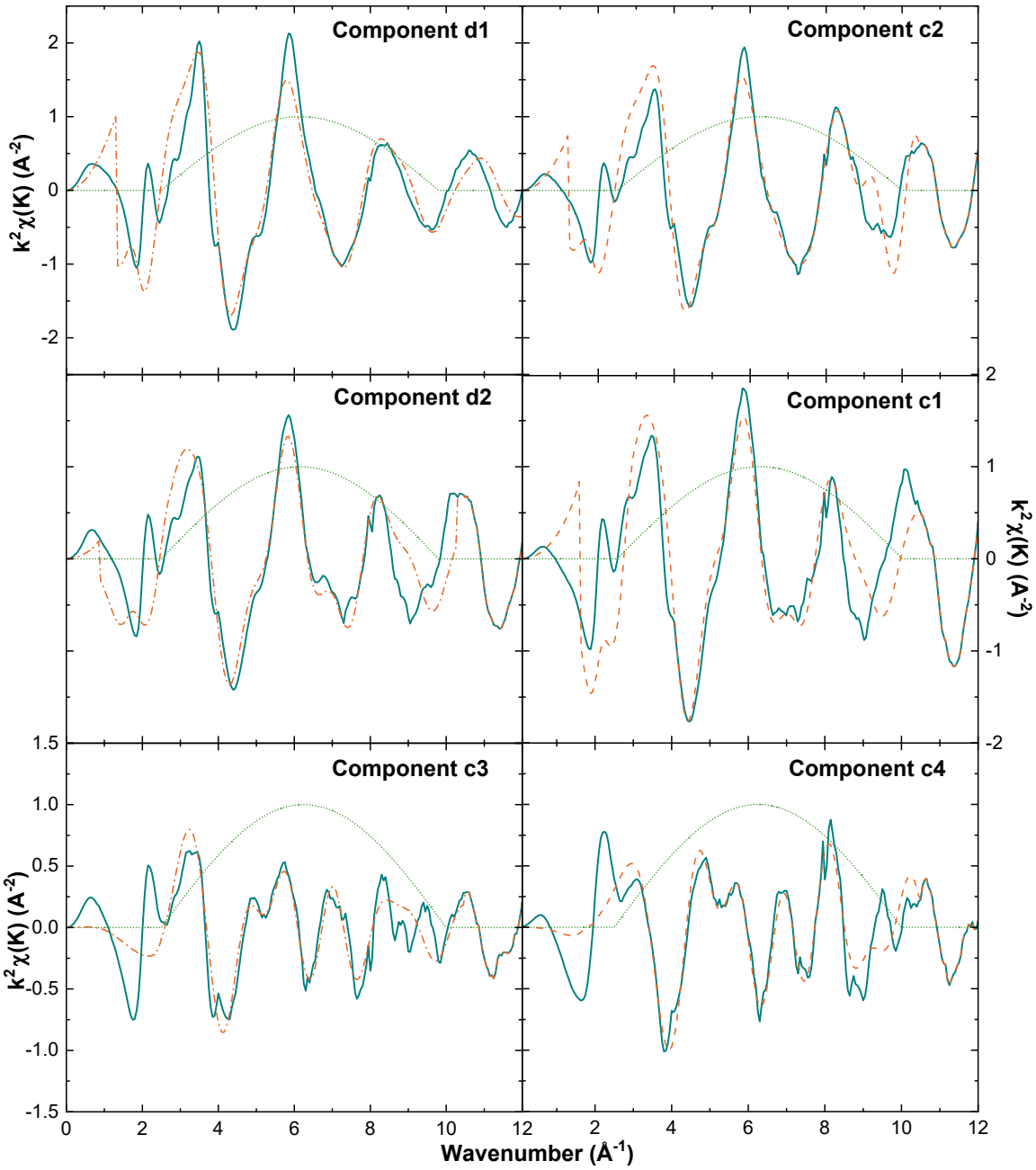

Figure S7: EXAFS fits of the pure components obtained from MCR-ALS analysis of the operando dataset shown in the k space.